Cellulose (2018) 25:4211–4222
https://doi.org/10.1007/s10570-018-1837-9

ORIGINAL PAPER

Imparting superhydrophobic and antibacterial properties onto the cotton fabrics: synergistic effect of zinc oxide nanoparticles and octadecanethiol

Nahid Ghasemi · Javad Seyfi · Mohammad Javad Asadollahzadeh

Received: 14 October 2017 / Accepted: 7 May 2018 / Published online: 10 May 2018

Abstract In this research, a one-step method for the preparation of superhydrophobic and antibacterial cotton fabric is presented, which has been modified by zinc oxide (ZnO) nanoparticles and octadecanethiol (ODT). The individual use of ZnO and ODT resulted in superhydrophilic fabrics whereas their combined use caused a transformation to the superhydrophobic behavior. Based on the morphological analysis, the distribution of ZnO nanoparticles on the fabrics' surfaces was notably improved leading to a much more uniform rough structure. Such proper level of roughness along with the hydrophobicity induced by ODT were found responsible for the observed high contact angle (161°). The deposition of ZnO and ODT on the fabrics' surfaces was further proved by X-ray photoelectron spectroscopy. The bacterial adhesion experiments revealed that even the sole presence of ODT could notably reduce the bacterial attachment to the fabric due to the reduced surface free energy. The individual use of ZnO nanoparticles was found to have a strong antibacterial effect on both *Staphylococcus aureus* (Gram-positive) and *Escherichia coli* (Gram-negative) bacteria. The bacterial adhesion was even further diminished upon the combined use of ZnO and ODT. The numbers of adhered *S. aureus* and *E. coli* cells were highly reduced from 438,000 and 192,000 CFU cm^{-2} for the pristine fabric to 600 and 48 CFU cm^{-2} for the superhydrophobic fabric, respectively. Simultaneous achievement of superhydrophobicity and antibacterial activity on the fabrics' surfaces could have promising potential in the hospital garments and facemasks where patients and staff need to be protected from the infections.

Keywords Antibacterial · Cotton fabric · Nanoparticles · Superhydrophobic

Introduction

The tremendous potential of superhydrophobic materials has made them extremely intriguing for researchers worldwide since they are being used in a vast range of applications such as self-cleaning, anti-biofouling, anti-adhesive and anti-icing surfaces (Fürstner et al. 2005; Suryaprabha and Sethuraman 2017; Seyfi et al. 2016; Hejazi et al. 2017). To fabricate superhydrophobic surfaces, the water contact angles (WCAs) above 150° and sliding angles (SAs) below 10° have to be

Electronic supplementary material The online version of this article (https://doi.org/10.1007/s10570-018-1837-9) contains supplementary material, which is available to authorized users.

N. Ghasemi · J. Seyfi (✉) · M. J. Asadollahzadeh
Department of Chemical Engineering, Islamic Azad University, Shahrood Branch,
P.O. Box 36155-163, Shahrood, Iran
e-mail: Jseyfi@gmail.com

achieved via tuning the surface roughness and chemical composition of the material's surface layer. A wide range of substrates have been used to fabricate superhydrophobic surfaces including sponges (Salehabadi et al. 2017), carbon steel (Xiang et al. 2017), filter paper (Piltan et al. 2016), and among them, fibrous substrates have been greatly studied due to their extensive applicability in various fields such as self-cleaning textiles (Zhu et al. 2017), oil–water separation (Yang et al. 2017), antibacterial textiles (Ivanova and Philipchenko 2012), and microfluidic transport (Xing et al. 2013). A diverse range of methods has been utilized to impart superhydrophobicity onto the commercial fabrics. For instance, Wang et al. (2016) fabricated superhydrophobic textile for oil–water separation through the immersion of the fabrics into a fly ash dispersion followed by hydrophobic modification. Another group has used an electrostatic layer-by-layer assembly of polyelectrolyte/nanosilica multilayers on cotton fabrics followed by a fluoroalkylsilane modification (Zhao et al. 2010). In another work, a superhydrophobic antibacterial textile was developed by spraying of fluorocarbon-modified chitosan nanoparticles dispersion over the textile samples (Ivanova and Philipchenko 2012). As mentioned, a proper level of surface roughness and a very low surface free energy are required for achieving superhydrophobicity. Herein, the major challenge is to properly lower the surface free energy of the fabrics since they already possess a micrometer-scale roughness naturally originating from the fibers and the corresponding woven structure, and thus, only a single-scale nanostructure needs to be formed on the fibers. To this end, researchers have used a wide range of nano-materials such as carbon nanotubes (Hsieh et al. 2008), graphene oxide (Yan et al. 2016), zinc oxide nanorods (Xu and Cai 2008), and etc.

One of the outstanding features of superhydrophobicity is the greatly reduced bacterial adhesion on the surfaces of superhydrophobic materials. In fact, these surfaces have been recently considered as "antibacterial" due to their remarkable inhibiting effect on the bacterial adhesion without the use of any biocides (Zhang et al. 2013). Superhydrophobicity could diminish the adhesion force between bacteria and a solid surface leading to the effortless removal of bacteria before a thick biofilm is formed on the surface (Crick et al. 2011). Protein adsorption is majorly responsible for the bacterial adhesion process, which has been proved to be highly diminished on superhydrophobic surfaces leading to a reduced bacterial adhesion (Stallard et al. 2012).

As compared with organic antibacterial agents, inorganic metal oxides are more robust and exhibit higher stability and longer shelf life [20]. In both microscale and nanoscale formulations, zinc oxide (ZnO) is being increasingly investigated for its remarkable antibacterial activity and has a huge potential to be used in food and medical industries due to being nontoxic, biosafe and biocompatible (Raghupathi et al. 2011). In this work, ZnO nanoparticles with the size less than 50 nm were utilized since it has been reported that the smaller sized ZnO nanoparticles have higher antibacterial activity rather than the larger sized nanoparticles (Rosi and Mirkin 2005).

According to the literature, many of the proposed methods were rather elaborative or substrate restricted, and some of the simpler methods have used fluorinated materials to reduce the surface free energy. In the current research, a fluorine-free one-step method based on the dip coating technique is suggested to fabricate superhydrophobic cotton fabrics. ZnO nanoparticles were used to induce the nanoscale rough structure, and was found to play an essential role in achieving our main purposes, which are, superhydrophobicity and antibacterial property. Moreover, a surface free energy reducing agent, octadecanethiol (ODT), was employed to reduce the surface free energy of the fabrics. The major aim of this work was to design and produce the fabric with the highest superhydrophobicity and antibacterial activity which can have the potential to be used in surgical gowns and drapes, clean air suits, and facemasks in order to effectively reduce the risk of nosocomial infections. To the best of our knowledge, this is the first report on the synergistic effect of the combined use of ZnO nanoparticles and a surface free energy reducing agent such as ODT on the superhydrophobicity and antibacterial activity of the cotton fabrics.

Materials and methods

Materials

Zinc oxide nanoparticles with the size less than 50 nm and the surface area higher than 10 $m^2 g^{-1}$ was purchased from Sigma-Aldrich (St. Louis, MO, USA). Octadecanethiol (ODT) with a molecular weight of 286 g mol^{-1} and density of 0.847 g mL^{-1} was also obtained from Sigma-Aldrich. The cotton fabrics were supplied from the local market with the thickness of 0.4 mm and the weight per surface unit of 130 g m^{-2}. Chloroform was obtained from Merck (Darmstadt, Germany) and used as received.

Treatment process

A fixed amount of ODT (10 mg) and various contents of ZnO nanoparticles (10, 30 and 50 mg) were added to 10 mL of chloroform, and the suspension was vigorously mixed by magnet stirring for 2 h. Afterwards, the fabric samples (3 × 3 cm^2) were immersed into the as-prepared suspension for different dipping times (1, 5, 15, 30 and 60 min) while being gently stirred. After the preliminary tests, the optimal dipping time was introduced as 30 min, and thus, the final samples were all prepared at the dipping time of 30 min. The dipped fabrics were then removed from the suspension and dried at ambient conditions for 6 h to thoroughly evaporate the solvent. Based on the WCA measurements, 30 mg of ZnO was the optimum content of nanoparticles, and thus, another sample was treated with 30 mg of ZnO nanoparticles in the absence of ODT. Moreover, a sample was also prepared in the absence of nanoparticles, and only 10 mg of ODT was added to the chloroform. For comparison reasons, the optimum formulation (30 mg ZnO and 10 mg ODT) was also prepared by a two-step method. Firstly, the fabric samples were dip-coated within the ZnO dispersion, removed and left to dry. In the second stage, the ZnO coated fabric was immersed into an ODT solution. The formulation of the prepared samples is listed in Table 1.

Characterization

A video-based contact angle measurement system (OCA 15, DataPhysics Instruments GmbH, Germany) was used to determine the CAs of the samples. The CA measurement of each sample was carried out at least three times across the sample surface using the sessile drop method by dispensing 4 μL drops of de-ionized water on the samples' surfaces. All CA measurements were taken under ambient laboratory conditions at a temperature of about 25 C. Morphologies of the fabrics' surfaces were evaluated on a scanning electron microscope (KYKY-EM3200) operated at 25 kV. To increase the resolution for SEM observation, the samples were plated with gold coating in order to render them electrically conductive. X-ray photoelectron spectroscopy (XPS) analysis was performed by using XPS spectroscopy with a monochromatic AlK_α X-ray source (1486.6 eV photons), operated at 180 W (12 kV and 15 mA) and under ultra-high vacuum conditions. The mechanical properties of the pure and superhydrophobic samples were measured via a stress–strain test conducted by an Instron Universal Testing Machine (Model 5566, Instron Corporation, Canton, MA, USA) following the ASTM Standard Test Method D 882-91.

Bacterial growth conditions

In this study, to assess the interactions between the fiber surfaces with two types of gram positive and gram negative bacterial cell walls, *Staphylococcus aureus* and *Escherichia coli* were used, respectively. Bacteria cells were obtained in the freeze-dried form from Persian Type Culture Collection. Bacteria were sub-cultured onto tryptic soy agar (TSA; Sigma) for 36 h at 37 °C, and then, three colonies from the TSA were incubated in 15 mL of Tryptic soy broth (TSB) aerobically for 24 h at 37 °C on a rotary shaker (Lab-Line Lab Rotator, Barnstead International) at 120 rpm until the stationary phase culture was reached. Afterwards, to obtain early logarithmic phase cells, 1 mL of the culture suspension was inoculated into 30 mL of fresh TSB under the same conditions for 12 h. Cells were collected by centrifugation at 6500 rpm for 5 min, washed with 0.1 M phosphate-buffered saline (PBS; Sigma), pH = 7.4, and resuspended in 0.1 M PBS at a concentration of 108 colony-forming units (CFU) mL^{-1}, enumerated by plate count agar.

Bacterial adhesion assay

For evaluating the bacterial adhesion process, the sterilized samples with 2.5 cm diameter were attached

Table 1 The formulation of the prepared samples

Samples	Chloroform (mL)	ZnO (mg)	ODT (mg)	Process type
ODT	10	–	10	One-step
Zn30	10	30	–	One-step
Zn10–ODT	10	10	10	One-step
Zn30–ODT	10	30	10	One-step
Zn50–ODT	10	50	10	One-step
Two_step	10	30	10	Two-step

with carbon tape at the bottom of standard 24-well culture plates containing 1.5 mL of TSB enriched with 0.25% of glucose (Merck). After that, 50 μL of the bacterial suspension (10^8 bacteria mL^{-1}) were seeded into each well and incubated for 24 h at 37 °C in an orbital shaker (120 rpm). All the experiments were performed in triplicate, on three independent occasions. The samples were removed from the wells and washed twice with PBS to rinse away any non-adherent cells and loosely attached bacteria, and then, again placed in 0.5 mL TSB followed by ultrasonication in an ultrasonic cleaner (Medal W-375, Ultrasonics) at a frequency of 25 kHz for 10 min to remove the bacteria from the surfaces. The samples were then vortexed for 1 min, serially diluted and viable plate counting was performed to quantify the numbers of adherent bacteria in CFU cm^{-2}. In order to observe the attached bacteria by SEM analysis, the samples were washed three times with sterile PBS and then fixed in 2.5% glutaraldehyde in PBS for 24 h. After fixation, the samples were dehydrated by a 10 min immersion in water–ethanol solutions with increasing concentrations of ethanol up to 100% and finally placed in a sealed desiccator. After sputter coating with gold, the samples were detected by scanning electron microscopy.

Results and discussion

Wettability results

The wetting behavior of samples was investigated by contact angle (CA) measurement. The pristine fabric showed an utterly hydrophilic behavior such that the water droplet completely wetted its surface. At first, the ODT-treated and ZnO-treated fabrics were prepared to understand the sole effect of each material on the wetting behavior of the fabrics. It was observed that both surface treated fabrics were highly hydrophilic and completely absorbed the water droplets. However, the water absorption rate was in the following order: pristine fabric > ZnO-treated fabric > ODT-treated fabric. In fact, both ODT and ZnO could not significantly change the wetting behavior of the fabrics, and no hydrophobicity was attained.

Quite oppositely, the fabric's wettability was transformed from an utterly hydrophilic character into a very hydrophobic behavior upon treatment by a combination of ZnO and ODT at different compositions. Figure 1 demonstrates that the CA value for Zn10–ODT, treated with the lowest amount of nanoparticles, is 140°. However, this very high value is not the true CA of this sample since the water droplet completely wetted the fabric after several seconds, and thus, Zn10–ODT was regarded as ultra-hydrophilic because according to the literature, if only the water droplet wets the surface under the time period of 0.5 s, the surface would be regarded as superhydrophilic (Han et al. 2007).

Increasing the ZnO content from 10 to 30 mg (in 10 mL of chloroform) has resulted in a superhydrophobic property showing the CA of 161° and a sliding angle less than 2° indicating an absolutely self-cleaning behavior. It should be mentioned that the self-cleaning effect observed in this sample is based on the flow of water droplets on the surface leading to the efficient removal of dirt particles, and no photocatalytic self-cleaning was detected (Karimi et al. 2014). Most probably, increasing the nanoparticle content from 10 to 30 mg must have led to a complete coverage of the fabric's surface by ZnO particles. More importantly, the observed superhydrophobic behavior remained stable even after a long period of time until the water droplet was eventually evaporated. The high fragility of superhydrophobic surfaces to hand touch has been reported because the induced micro/nano structure to the surface is highly sensitive

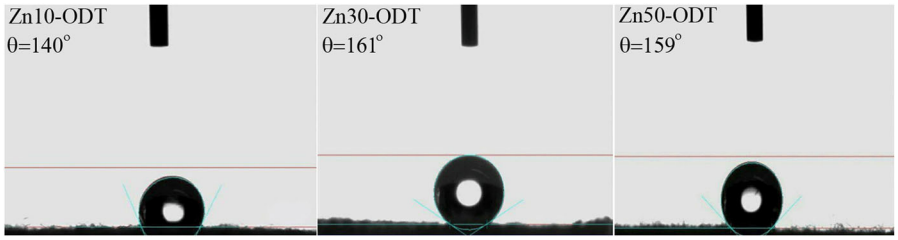

Fig. 1 The water drop profiles and water contact angles for the treated fabrics

to even small abrasion forces (Verho et al. 2011). It should be noted that the treated fabric in the case of Zn30–ODT sample retains its superhydrophobicity even after a severe finger touch. Despite its resistance to the severe finger touch, the durability of the superhydrophobic fabric was also studied under severe washing conditions. To this end, the Zn30–ODT sample was stirred in aqueous solution of laundry detergent (500 rpm, 10 mL laundry detergent in 50 mL ultrapure water) for 24 h, and then, the CA values were measured. Based on the results shown in Table S1, the sample retains its superhydrophobic property after 24 h of washing; however, the CA was reduced to 151° and the SA was increased to 20° indicating a slight reduction in the hydrophobicity of the fabric. Moreover, the mechanical properties of the pure fabric and Zn30–ODT are reported in Table S2. As could be anticipated, the mechanical properties of the fabric were not significantly changed, and only a slight enhancement in the tensile strength and modulus and an insignificant decline in the elongation at break were observed upon introducing the ZnO and ODT. The reason for such insignificant influence on the mechanical properties of the fabric could be attributed to the fact that only the outmost layer of the fabric has been modified by a nanoscale coating. Moreover, it can be inferred that the used modification method had no adverse effect on the structure and texture of the fabric.

An insignificant reduction in the CA value of the fabric was observed once the ZnO content increased to 50 mg indicating that the superhydrophobicity is retained even at a higher loading of nanoparticles. However, due to the lower nanoparticle requirement and higher WCA value, the Zn30–ODT is introduced as the optimum sample.

For comparison reasons, Zn30–ODT sample was also prepared by a different route upon which the treatment process was conducted in two steps. Quite interestingly, the water droplet was observed to be totally absorbed by the Two_step sample. It may be inferred that the one-step process caused more strong interactions to be formed between the ZnO particles and ODT molecules. The possible reason for this phenomenon will be further discussed by morphology results. It also should be noted that no discernible change was detected in the color of the fabrics upon modifying by ZnO and ODT.

SEM results

To better delineate the reasons for the interesting wetting results, scanning electron microscopy (SEM) was utilized. Figure 2a, b show the surface morphology of the pristine fabric at two different magnifications. It is seen that the average diameter of the fibers is around 20 μm. Figure 2c depicts the surface morphology of ODT-treated sample. It could be inferred that the surface of fibers in the case of the ODT-treated sample is nearly smooth and only some aggregations in the nano-scale are hardly detectable at some spots on the surface of fibers. Therefore, a proper level of surface roughness cannot be expected from the ODT-treated fabric. On the other hand, Fig. 2d–f illustrate the surface morphologies of Zn30 in which the ODT is absent. Figure 2e clearly shows that the fabric's surface was severely coated by ZnO nanoparticles, and thus, a very rough structure has been formed on the surface of Zn30. However, due to the formation of agglomerations at some spots, the rough structure was not evenly distributed. The role of surface roughness uniformity on achieving superhydrophobicity and self-cleaning behavior has been previously emphasized in our previous publications (Bolvardi et al. 2017; Seyfi et al. 2015). Having said that, it has to be noted that the surface energy of Zn30 has been quite high due to the absence of any hydrophobic surface modifications. In the literature, numerous publications reported the use of surface energy reducing agents along with nanoparticles to achieve

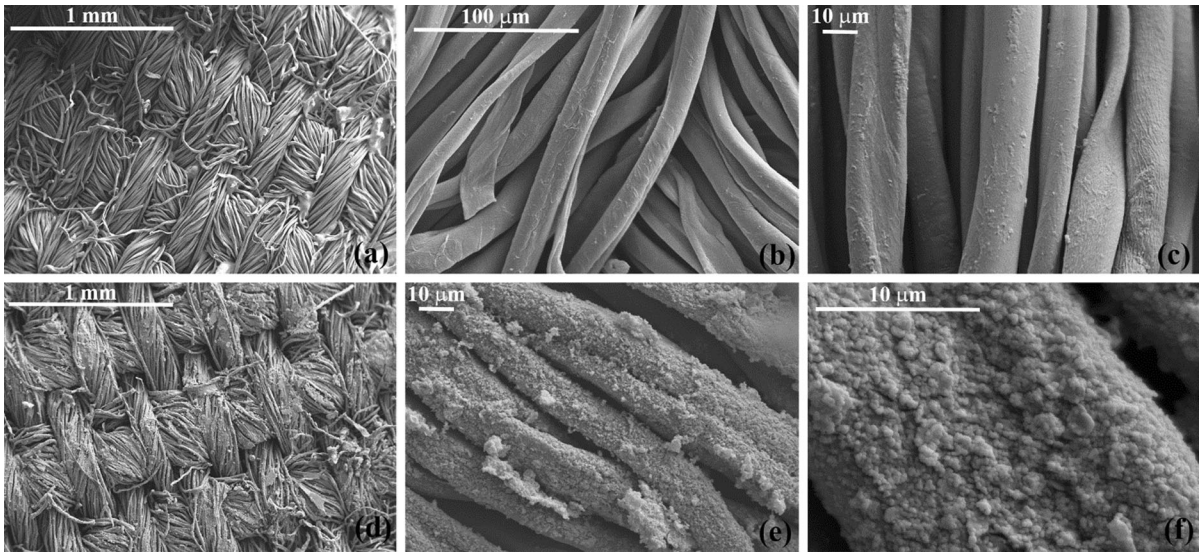

Fig. 2 SEM images from the surfaces of **a**, **b** pristine fabric at magnifications of × 50 and × 500, **c** ODT-treated fabric at magnification of × 1000, and **d**–**f** Zn30 sample at magnifications of × 50, × 1000 and × 5000

superhydrophobicity. It is well-established that a proper level of roughness along with a sufficiently low surface energy could result in a superhydrophobic character (Esmaeilpour et al. 2016). Based on Wenzel model, an intrinsically hydrophilic surface would become superhydrophilic if a proper level of roughness is induced on the material's surface (Wenzel 1936). Figure 2f further demonstrates the as-formed packed structure of ZnO nanoparticles on the surface of a fiber.

Figure 3 illustrates the surface morphologies of the fabrics treated with a combination of ZnO and ODT. Based on Fig. 3a, an utterly uniform distribution of nanoparticles could be observed throughout the whole fabric's surface; however, the higher magnification image shown in Fig. 3b indicates the formation of disperse rough structure on the surface of fibers due to the low content of used nanoparticles. The maximum size of ZnO clusters reaches 2 μm but the distance between the clusters exceeds several micrometers at some spots suggesting that the surface layer of fibers is not completely covered by nanoparticles. According to the wetting results, the initial CA for this sample was measured as 140° but after a few seconds, the water droplet was thoroughly absorbed by the fabric.

Figure 3c, d evidently shows that further increment of ZnO content resulted in a remarkable change in the surface morphology, and as a result, an utterly packed structure has been formed. In fact, the ZnO clusters were more adhered to each other forming an ordered and uniform rough structure. One could state that all the necessary prerequisites for a self-cleaning behavior are provided in the case of Zn30–ODT. First of all, the level of surface roughness is suitably high due to the formation of ZnO clusters on the surface layer of the sample. Secondly, the induced rough structure is notably uniform throughout the whole fabric's surface, and finally, the surface energy of sample must have been greatly diminished by using a proper amount of a surface energy reducing agent (ODT).

Another important observation could be made by comparing the SEM images of Zn30–ODT (Fig. 3c) and Zn30 (Fig. 2e). It could be realized that the addition of ODT to the formulation has resulted in a much more uniform surface morphology impeding the formation of agglomerations. It could be claimed that ODT molecules have facilitated the dispersion of ZnO nanoparticles within the solution which could impede the formation of agglomerations at the fabric's surface after evaporation of the solvent.

Figure 3e demonstrates that increasing the exceedingly high amount of ZnO nanoparticles caused the surface rough structure to be more coarsened as compared with Zn30–ODT. The distribution of ZnO clusters is still satisfactory and just a few agglomerations could be detected on the surface layer which is

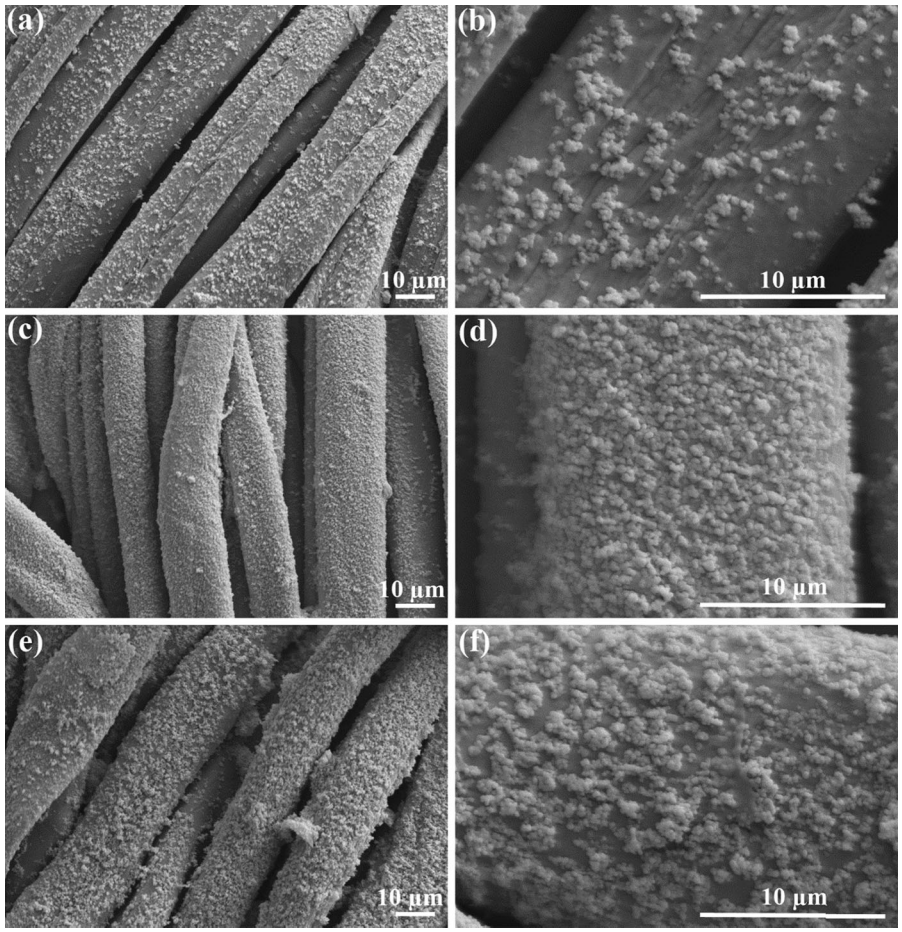

Fig. 3 SEM images from the surfaces of **a**, **b** Zn10–ODT, **c**, **d** Zn30–ODT, and **e**, **f** Zn50–ODT at magnifications of × 1000 and × 5000

quite expected since a high concentration of nanoparticles was used in that sample (5 mg mL^{-1}).

As mentioned in the previous section, the optimum formulation was also prepared by a two-step method to compare the effect of preparation process on the final wetting behavior. The surface morphology of the sample made by two-step method is shown in Fig. 4. Comparing Figs. 4a, b and 3c, d leads one to conclude that the treatment process has a remarkable influence on the surface morphology of the fabrics. Quite surprisingly, the wetting behavior was shifted from superhydrophobic in the case of the one-step method to superhydrophilic in the case of the two-step method. According to the obtained SEM images, one could infer that the incomplete coverage of the fabric's surface was mainly responsible for the observed shift in the wetting behavior.

XPS results

In order to prove the efficient deposition of ZnO and ODT on the surfaces of fabrics, X-ray photoelectron spectroscopy (XPS) was utilized to determine the elemental composition of the surface layer of samples. To this end, the pristine fabric, the ODT-treated fabric and the fabric treated with the optimum formulation (Zn30–ODT) were analyzed by XPS. In the wide-scan spectrum of the untreated fabric (the middle spectrum in Fig. 5), two distinguished peaks could be observed at binding energies of 285 and 532 eV which correspond to carbon and oxygen, respectively. This result was anticipated since the pristine fabric is utterly made of cellulose.

The atomic percentages of different elements were calculated based on the area under the peaks and

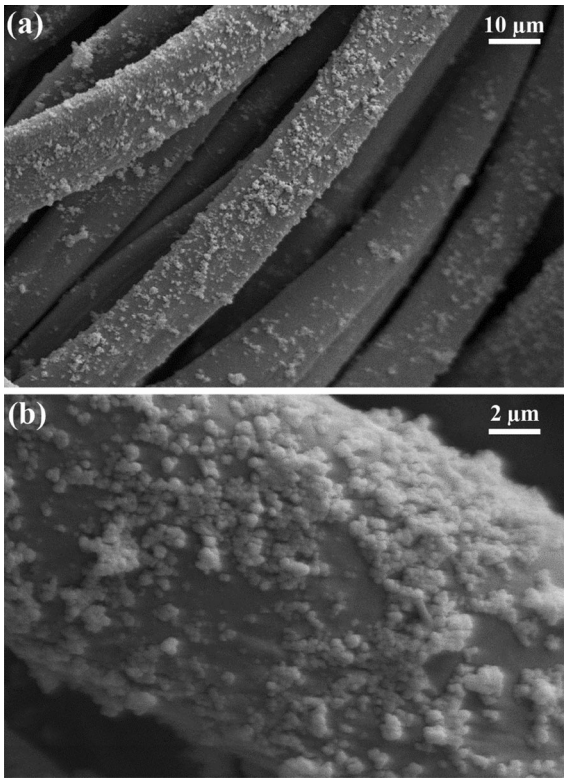

Fig. 4 The surface morphology of Two_step sample at magnifications of **a** × 1000 and **b** × 5000

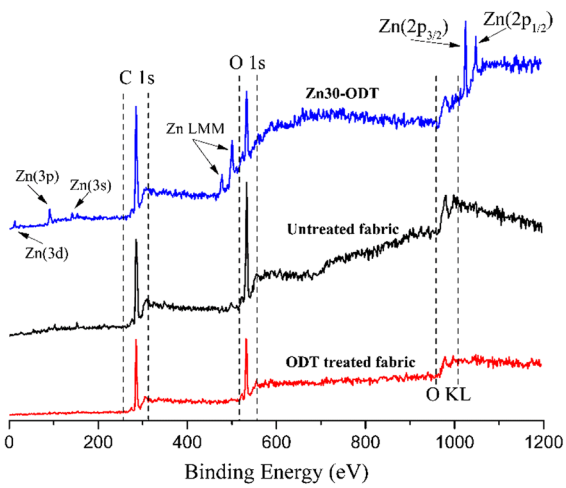

Fig. 5 The wide-scan XPS spectra for the untreated fabric, and the fabrics treated with ODT and ZnO

reported in Table 2. As can be seen, the surface of the pristine fabric is equally made of carbon and oxygen, and the ratio of carbon to oxygen is 0.96. Once the fabric is treated by ODT, it is seen that the [C]/[O] ratio is increased from 0.96 to 1.14 which could be attributed to the presence of ODT chains on the surface of the fabrics. Due to the molecular structure of ODT, $CH_3(CH_2)_{16}CH_2SH$, which has 18 carbon atoms and zero oxygen atoms, the [C]/[O] ratio is increased on the surface of ODT-treated fabric further proving that ODT was successfully deposited on the fabrics' surfaces.

In contrast with the pristine fabric and the ODT-treated fabric, which exhibited rather similar XPS wide-scan spectra, the Zn30–ODT treated fabric shows a totally different XPS spectrum. In addition to the variations in the intensity of C1 *s* and O1 *s* peaks, several other peaks also appeared all of which are ascribed to the zinc atoms. The peaks appeared at binding energies of 1028 and 1051 eV are related to Zn($2p_{3/2}$) and Zn($2p_{1/2}$), respectively. Two distinct peaks around the binding energies of 479 and 499 eV are due to the oxygen vacancies on the ZnO particles (Zn LMM). As can be seen in the XPS spectra of Zn30–ODT treated fabric, the Zn 2*p* peaks are very pronounced implying the strong presence of ZnO nanoparticles at the surface layer of the optimum sample. The quantified results also prove that the surface layer is mainly composed of ZnO particles since a very high atomic concentration was obtained for the zinc atom (30.7%). Obviously, the cellulose chains were less detected by XPS due to the coverage of the surface by ZnO nanoparticles. Having said that, the carbon concentration is still rather high (42.5%) the majority of which could be attributed to the ODT chains present at the surface layer of the fabric since the ratio of [C]/[O] was notably increased to 1.58. This claim could be further corroborated if one considers the fact that the majority of detected oxygen atoms (26.8%) belong to the ZnO nanoparticles, not the cellulose chains.

Bacterial adhesion results

Firstly, the attachment of both Gram-positive and Gram-negative bacteria on the surface of the pristine fabric and the superhydrophobic sample (Zn30–ODT) is investigated by SEM analysis. Figure 6 shows the surface morphology of the pristine fabric and the superhydrophobic sample after 24 h of incubation. Quite expectedly, Fig. 6a, b clearly demonstrate the colonization of *S. aureus* bacteria on the surface of the pristine fabric. The higher magnified image seen in

Table 2 The quantified XPS results for several samples

Samples	[C] (%)	[O] (%)	[Zn] (%)	[C]/[O]
Untreated fabric	49.15	50.85	–	0.96
ODT-treated fabric	53.4	46.6	–	1.14
Zn30–ODT treated fabric	42.5	26.8	30.7	1.58

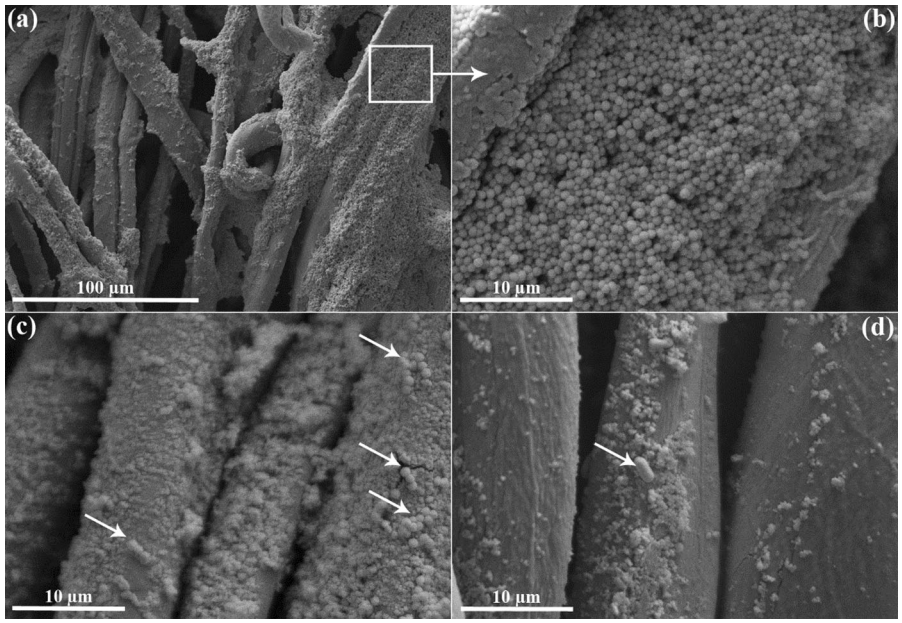

Fig. 6 SEM images of *S. aureus* on the surfaces of **a**, **b** the pristine fabric and **c** Zn30–ODT treated fabric, and *E. coli* on the surface of **d** Zn30–ODT treated fabric at incubation time of 24 h

Fig. 6b evidently proves that the *S. aureus* bacteria have been severely colonized on the whole surface of the fiber, and their shape is spherical exhibiting an average diameter of 1 µm. As can be seen in Fig. 6c, the surface of the superhydrophobic sample was remarkably more resistant to *S. aureus* as compared with the pristine fabric since only a few cells could be observed which were marked in the figure. Based on Fig. 6d, it can be seen that the resistance to the bacterial attachment is even further increased in the case of *E. coli* since much fewer cells were observed attached on the fabrics based on a large scanned area. These qualitative results imply the fact that the superhydrophobic sample exhibited an outstanding antibacterial activity against both Gram-positive and Gram-negative bacteria.

Apart from the qualitative analysis of the bacterial adhesion, the number of adhered cells on the surface of several samples were measured to quantitatively study the bacterial adhesion as well. Figure 7 depicts the number of adhered cells (CFU cm^{-2}) after 24 h of incubation for samples with different compositions and thus wettabilities. The first observation is that the Gram-positive bacteria were more adhered on the surface of the pristine fabric as compared with the Gram-negative bacteria. Such remarkably lower adhesion of *E. coli* with respect to the *S. aureus* ($\sim$ 56%) could be explained by both geometrical and chemical factors. Apart from the considerably different composition of the cell wall of Gram-positive and Gram-negative bacteria (Poortinga et al. 2002), it should be reminded that *S. aureus* is a spherical coccus (diameter less than 1 µm) and *E. coli* is a cylindrical bacillus (width $\sim$ 0.5 µm and length $\sim$ 2 µm). Therefore, it is likely that the spherical bacteria would need a much lower degree of surface contact to allow successful

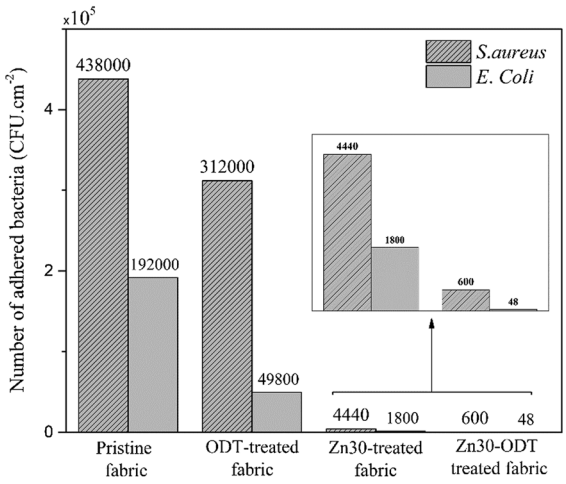

Fig. 7 The number of adhered bacteria for both *S. aureus* and *E. coli* bacteria after 24 h of incubation

adhesion compared to the rod-shaped bacteria (Fadeeva et al. 2011).

Quite interestingly, a reduced bacterial adhesion is observed for the ODT-treated fabric as compared with the pristine fabric for both types of bacteria. Such result indicates that the presence of a low surface free energy material on the fabric's surface is rather influential on the bacterial adhesion. Herein, and according to the SEM results (Fig. 2c), the geometrical factors are negligible, and instead, the chemical factors are majorly responsible for the reduced bacterial adhesion. It also should be reminded that both pristine and ODT-treated fabrics exhibited the CA $\sim 0°$, and thus, the reduced bacterial attachment could be attributed to the lower water absorption rate in the case of ODT-treated fabric which is originated from the lowered surface free energy.

According to Fig. 7, the numbers of adhered *S. aureus* and *E. coli* cells have been decreased from 430,000 and 192,000 CFU cm^{-2} for the pristine fabric to 4440 and 1800 CFU cm^{-2} for the Zn30-treated fabric. Such striking decline in bacterial adhesion for Zn30-treated fabric has to be attributed to the antibacterial character of ZnO nanoparticles. One of the suggested mechanisms for the antibacterial behavior of ZnO nanoparticles is their surface abrasiveness which has been reported to produce disorganization of both cell wall and cell membrane of *E. coli* (Padmavathy and Vijayaraghavan 2008). Another suggested mechanism is based on the deposition of the nanoparticles on the surface of bacteria or accumulation of nanoparticles either in the cytoplasm or in the periplasmic region which could lead to the disruption of cellular function (Raghupathi et al. 2011; Brayner et al. 2006).

The highest degree of antibacterial behavior was observed in the case of the superhydrophobic sample (Zn30–ODT treated fabric). The inset in Fig. 7 shows the differences in the bacterial adhesion of Zn30 and Zn30–ODT samples more clearly. The numbers of adhered *S. aureus* and *E. coli* cells were reduced from 4440 and 1800 CFU cm^{-2} in the case of Zn30 treated fabric to 600 and 48 CFU cm^{-2} in the case of Zn30–ODT treated fabric. The further reductions observed in the bacterial adhesions could be majorly ascribed to the notably reduced surface free energy of the fabric as a result of the presence of ODT. It could be concluded that the use of a surface free energy reducing agent alone cannot guarantee an effective antibacterial property (ODT-treated fabric); however, if accompanied by a proper level of rough structure, a significant antibacterial behavior would be expected.

It is also noteworthy that the superhydrophobic sample follows the Cassie–Baxter regime based on which a superhydrophobic behavior with ultra-low sliding angles can be obtained thanks to the air entrapment inside the surface pores and cavities, which increases the solid–vapor interface (Cassie and Baxter 1944). Based on the literature, the air-trapping ability of a Cassie-Baxter state, which leads to an *anti*-bioadhesive property, could greatly reduce the adhesion of different strains of bacteria (Bruzaud et al. 2017; Freschauf et al. 2012; Qian et al. 2017). In the current study, it can be inferred that, apart from the remarkably reduced surface free energy and the obtained Cassie-Baxter state, the uniformity of surface rough structure was enhanced upon addition of ODT to the Zn30 formulation which also might be one of the reasons for the further reduced bacterial adhesion.

Another interesting observation from Fig. 7 is that the adhesion of *E. coli* cells was more inhibited as compared with that of *S. aureus* upon the transformation to a superhydrophobic state. It is true that the total surface area of the fabric increased as a result of the ZnO deposition, but the available surface area for cell adhesion is notably decreased due to the nano-scale distances formed between the surface rough features which are significantly smaller than the size of *E. coli* and *S. aureus* bacteria. It has been previously suggested that the bacterial adhesion to substrates

requires the presence of an appreciable amount of initial cellular contact with the surface (Fadeeva et al. 2011), and thus, it could be speculated that such initial cellular contact is less available for the *E. coli* bacteria due to its larger size with respect to the *S. aureus*.

Conclusion

Superhydrophobic and antibacterial cotton fabric treated with ZnO nanoparticles and octadecanethiol was prepared via a one-step dip coating technique. The individual utilizations of ZnO and ODT in preparation of the surface treated fabrics resulted in a superhydrophilic behavior similar to the pristine fabric; however, the rate of water absorption was different which was attributed to the variation in the surface free energy of the samples. Once a combination of ZnO and ODT was utilized in the surface treatment of the fabrics, it was found that the uniformity of the morphology was notably improved, and the wetting behavior was shifted from superhydrophilic to superhydrophobic since a proper level of roughness along with a low surface energy were provided in the case of the optimum sample (Zn30–ODT). The XPS analysis proved that ZnO was efficiently deposited on the surface of the fabrics. The SEM results from the adhered cells demonstrated that the pristine fabric was severely colonized by *S. aureus* cells while the superhydrophobic sample exhibited a remarkably lower level of *S. aureus* and *E. coli* adhesion on its surface. The number of adhered cells was also measured and the results showed that the *S. aureus* and *E. coli* cells were reduced from 438,000 and 192,000 CFU cm^{-2} for the pristine fabric to 600 and 48 CFU cm^{-2} for the superhydrophobic sample, respectively. Such strong antibacterial property was attributed to the role of ZnO nanoparticles in killing the bacteria via their surface abrasiveness and also accumulation on the surface of bacteria leading to disorganization of the cells. Moreover, the role of the trapped air on the surface of the fabric and its anti-bioadhesive property was highlighted in inhibition of the cell adhesion on the surface of the superhydrophobic sample.

Acknowledgments Partial financial support from the Iranian Nanotechnology Initiative is gratefully appreciated.

Compliance with ethical standards

Conflict of interest The authors declare that they have no conflict of interest.

References

Bolvardi B, Seyfi J, Hejazi I, Otadi M, Khonakdar HA, Drechsler A, Holzschuh M (2017) Assessment of morphology, topography and chemical composition of water-repellent films based on polystyrene/titanium dioxide nanocomposites. Appl Surf Sci 396:616–624

Brayner R, Ferrari-Iliou R, Brivois N, Djediat S, Benedetti MF, Fievet F (2006) Toxicological impact studies based on *Escherichia coli* bacteria in ultrafine ZnO nanoparticles colloidal medium. Nano Lett 6:866–870

Bruzaud J, Tarrade J, Celia E, Darmanin T, Taffin de Givenchy E, Guittard F, Herry JM, Guilbaud M, Bellon-Fontaine MN (2017) The design of superhydrophobic stainless steel surfaces by controlling nanostructures: a key parameter to reduce the implantation of pathogenic bacteria. Mater Sci Eng C 73:40–47

Cassie ABD, Baxter S (1944) Wettability of porous surfaces. Trans Faraday Soc 40:546–550

Crick CR, Ismail S, Pratten J, Parkin IP (2011) An investigation into bacterial attachment to an elastomeric superhydrophobic surface prepared via aerosol assisted deposition. Thin Solid Films 519:3722–3727

Esmaeilpour M, Niroumand B, Monshi A, Ramezanzadeh B, Salahi E (2016) The role of surface energy reducing agent in the formation of self-induced nanoscale surface features and wetting behavior of polyurethane coatings. Prog Org Coat 90:317–323

Fadeeva E, Truong VK, Stiesch M, Chichkov BN, Crawford RJ, Wang J, Ivanova EP (2011) Bacterial retention on superhydrophobic titanium surfaces fabricated by femtosecond laser ablation. Langmuir 27:3012–3019

Freschauf LR, McLane J, Sharma H, Khine M (2012) Shrink-induced superhydrophobic and antibacterial surfaces in consumer plastics. PLoS ONE 7:40987

Fürstner R, Barthlott W, Neinhuis C, Walzel P (2005) Wetting and self-cleaning properties of artificial superhydrophobic surfaces. Langmuir 21:956–961

Han JT, Kim S, Karim A (2007) UVO-tunable superhydrophobic to superhydrophilic wetting transition on biomimetic nanostructured surfaces. Langmuir 23:2608–2614

Hejazi I, Seyfi J, Sadeghi GMM, Jafari SH, Khonakdar HA, Drechsler A, Davachi SM (2017) Investigating the interrelationship of superhydrophobicity with surface morphology, topography and chemical composition in spray-coated polyurethane/silica nanocomposites. Polymer 128:108–118

Hsieh CT, Chen WY, Wu FL (2008) Fabrication and superhydrophobicity of fluorinated carbon fabrics with micro/-nanoscaled two-tier roughness. Carbon 46:1218–1224

Ivanova NA, Philipchenko AB (2012) Superhydrophobic chitosan-based coatings for textile processing. Appl Surf Sci 263:783–787

Karimi L, Yazdanshenas ME, Khajavi R, Rashidi A, Mirjalili M (2014) Using graphene/TiO_2 nanocomposite as a new route for preparation of electroconductive, self-cleaning, antibacterial and antifungal cotton fabric without toxicity. Cellulose 21:3813–3827

Padmavathy N, Vijayaraghavan R (2008) Enhanced bioactivity of ZnO nanoparticles—an antimicrobial study. Sci Technol Adv Mater 9:035004

Piltan S, Seyfi J, Hejazi I, Davachi SM, Khonakdar HA (2016) Superhydrophobic filter paper via an improved phase separation process for oil/water separation: study on surface morphology, composition and wettability. Cellulose 23:3913–3924

Poortinga AT, Bos R, Norde W, Busscher HJ (2002) Electric double layer interactions in bacterial adhesion to surfaces. Surf Sci Rep 47:1–32

Qian H, Li M, Li Z, Lou Y, Huang L, Zhang D, Xu D, Du C, Lu L, Gao J (2017) Mussel-inspired superhydrophobic surfaces with enhanced corrosion resistance and dual-action antibacterial properties. Mater Sci Eng C 80:566–577

Raghupathi KR, Koodali RT, Manna AC (2011) Size-dependent bacterial growth inhibition and mechanism of antibacterial activity of zinc oxide nanoparticles. Langmuir 27:4020–4028

Rosi NL, Mirkin CA (2005) Nanostructures in biodiagnostics. Chem Rev 105:1547–1562

Salehabadi S, Seyfi J, Hejazi I, Davachi SM, Naeini AH, Khakbaz M (2017) Nanosilica-decorated sponges for efficient oil/water separation: role of nanoparticle's type and concentration. J Mater Sci 52:7017–7027

Seyfi J, Hejazi I, Jafari SH, Khonakdar HA, Sadeghi GMM, Calvimontes A, Simon F (2015) On the combined use of nanoparticles and a propersolvent/non-solvent system in preparation of superhydrophobic polymer coatings. Polymer 56:358–367

Seyfi J, Hejazi I, Jafari SH, Khonakdar HA, Simon F (2016) Enhanced hydrophobicity of polyurethane via non-solvent induced surface aggregation of silica nanoparticles. J Colloid Interface Sci 478:117–126

Stallard CP, McDonnell KA, Onayemi OD, O'Gara JP, Dowling DP (2012) Evaluation of protein adsorption on atmosphere plasma deposited coatings exhibiting superhydrophilic to superhydrophobic properties. Biointerphases 7:31

Suryaprabha T, Sethuraman MG (2017) Fabrication of copper-based superhydrophobic self-cleaning antibacterial coating over cotton fabric. Cellulose 24:395–407

Verho T, Bower C, Andrew P, Franssila S, Ikkala O, Ras RHA (2011) Mechanically durable superhydrophobic surfaces. Adv Mater 23:673–678

Wang J, Han F, Zhang S (2016) Durably superhydrophobic textile based on fly ash coating for oil/water separation and selective oil removal from water. Sep Purif Technol 164:138–145

Wenzel RN (1936) Resistance of solid surfaces to wetting by water. Ind Eng Chem 28:988–994

Xiang T, Ding S, Li C, Zheng S, Hu W, Wang J, Liu P (2017) Effect of current density on wettability and corrosion resistance of superhydrophobic nickel coating deposited on low carbon steel. Mater Des 114:65–72

Xing S, Jiang J, Pan T (2013) Interfacial microfluidic transport on micropatterned superhydrophobic textile. Lab Chip 13:1937–1947

Xu B, Cai ZS (2008) Fabrication of a superhydrophobic ZnO nanorod array film on cotton fabrics via a wet chemical route and hydrophobic modification. Appl Surf Sci 254:5899–5904

Yan H, Zhou H, Ye Q, Wang X, Cho CM, Yan A, Tan X, Xu J (2016) Engineering polydimethylsiloxane with two-dimensional graphene oxide for an extremely durable superhydrophobic fabric coating. RSC Adv 6:66834–66840

Yang W, Li J, Zhou P, Zhu L, Tang H (2017) Superhydrophobic copper coating: switchable wettability, on-demand oil-water separation, and antifouling. Chem Eng J 327:849–854

Zhang X, Wang L, Levänen E (2013) Superhydrophobic surfaces for the reduction of bacterial adhesion. RSC Adv 3:12003–12020

Zhao Y, Tang Y, Wang X, Lin T (2010) Superhydrophobic cotton fabric fabricated by electrostatic assembly of silica nanoparticles and its remarkable buoyancy. Appl Surf Sci 256:6736–6742

Zhu C, Shi J, Xu S, Ishimori M, Sui J, Morikawa H (2017) Design and characterization of self-cleaning cotton fabrics exploiting zinc oxide nanoparticle-triggered photocatalytic degradation. Cellulose 24:2657–2667